sustainability

MDPI

Article

Intelligent Optimized Wind Turbine Cost Analysis for Different Wind Sites in Jordan

Ayman Al-Quraan * and Bashar Al-Mhairat

Electrical Power Engineering Department, Hijjawi Faculty for Engineering Technology, Yarmouk University, Irbid 21163, Jordan; 2018979003@ses.yu.edu.jo

* Correspondence: aymanqran@yu.edu.jo

Abstract: Choosing the right wind site and estimating the extracted energy of the wind turbines are essential to successfully establishing a wind farm in a specific wind site. In this paper, a method for estimating the extracted energy of the wind farms using several mathematical models is proposed. The estimating method, which was based on five wind turbines, Q_1, Q_2, Q_3, Q_4, and Q_5 and three wind distribution models, gamma, Weibull, and Rayleigh, was used to suggest suitable specifications of a wind turbine for a specific wind site and maximize the extracted energy of the proposed wind farm. An optimization problem, developed for this purpose, was solved using the whale optimization algorithm (WOA). The suggested method was tested using several potential wind sites in Jordan. The proposed wind farms at these sites achieved the maximum extracted energy, maximum capacity factor (*CF*), and minimum levelized cost of energy (*LCoE*) based on the solution of the developed optimization problem. The developed model with Q_3 and the Rayleigh distribution function was validated with real measurement data from several wind farms in Jordan. Error analysis showed that the difference between the measured and estimated energy was less than 20%. The study validated the provided model, which can now be utilized routinely for the assessment of wind energy potential at a specific wind site.

Keywords: wind energy; wind turbine; power density; power–speed curve; probability distribution function

check for updates

Citation: Al-Quraan, A.; Al-Mhairat, B. Intelligent Optimized Wind Turbine Cost Analysis for Different Wind Sites in Jordan. *Sustainability* **2022**, *14*, 3075. https://doi.org/10.3390/su14053075

Academic Editors: María Del P. Pablo-Romero, Rafael Pozo-Barajas and Javier Sánchez-Rivas García

Received: 24 January 2022
Accepted: 1 March 2022
Published: 6 March 2022

Publisher's Note: MDPI stays neutral with regard to jurisdictional claims in published maps and institutional affiliations.

Copyright: © 2022 by the authors. Licensee MDPI, Basel, Switzerland. This article is an open access article distributed under the terms and conditions of the Creative Commons Attribution (CC BY) license (https://creativecommons.org/licenses/by/4.0/).

1. Introduction

Throughout history, humanity has always strived to maximize the utilization of natural resources. A good illustration of how this has been accomplished is through renewable energy resources. Renewable energy has become an urgent and critical requirement to address the concerns caused by using fossil fuels.

Wind power is now the most cost-competitive technology all over the world. In particular, the global wind sector hit a new high in 2017 [1]. This increase in wind capacity was attributed to a number of factors by the Global Wind Energy Council (GWEC), including (a) the introduction and deployment of a new generation of turbines with a larger shelf area and thus higher production; (b) increasing investor confidence; (c) technology and management improvement; and (d) industry maturity.

Wind speed and direction cannot be predicted precisely because of wind's stochastic nature [2]. The natural behavior of wind at a prospective site must be observed and evaluated to identify wind characteristics. Once the wind characteristics have been recognized, the components of the wind energy conversion system (WECS) can be efficiently developed. As a result, a wind energy assessment procedure can be completed flawlessly [3].

In general, evaluating wind resources involves four processes. The first stage entails measuring and gathering wind data from meteorological stations or airports. Wind data are often recorded every ten minutes at a height of 10 m, which is considered standard. The second stage comprises utilizing statistical distribution models to analyze the collected

data in order to establish the frequency distribution of average wind velocity for the candidate site over a certain time period. Each distribution model has a set of parameters that must be assigned using a combination of numerical approaches and optimization algorithms. By comparing the available distribution models, the best distribution function can be determined. Several goodness of fit indices, such as root mean square error (RMSE), coefficient of determination (R^2), and others, are used to do this. The distribution model can be depicted using a probability distribution function (PDF). The distribution function and the PV curve are used to analyze the wind energy that could be extracted from a certain wind turbine existing in a potential wind site. At the completion of this stage, a judgment can be made as to whether a wind turbine can be installed/or not in a certain wind site.

Many parametric distribution models have been used to evaluate wind energy resources, including the Weibull [4–18], Rayleigh [10–12,14–19], gamma [5,10], log-normal [10,13], log-logistic [13], and other distributions. The Weibull distribution has been used by the majority of researchers. In [10], Jiang et al. compared the Weibull distribution to the Rayleigh, gamma, and log-normal distributions to assess the energy potential of low wind speeds in China. When optimization methods were applied to find its parameters, the Weibull distribution was the best option. Wang et al., in [11], determined the Weibull model to be the best acceptable distribution among the five chosen distribution models after examining it using the RMSE. Wu et al., in [13], employed the Weibull, log-logistic, and log-normal distributions to estimate wind energy at typical sites in Inner Mongolia and China. The log-logistic and log-normal distributions performed better than the Weibull distribution, which had the lowest results. The authors in [14] presented a detailed review of 46 publications published between 2010 and 2018. In this investigation, the Weibull distribution was found to be superior (44 out of the 46 studies used the Weibull distribution). In [20], Li et al. compared the characteristics of onshore and offshore wind, as well as their wind energy potentials, in two locations along China's southeast coast. The data showed that offshore wind energy was more available than onshore wind energy, and the authors confirmed the accuracy of applying the Weibull distribution for both onshore and offshore wind energy. In [21], Bilir et al. employed the Weibull distribution to analyze power density based on wind data collected over a year from a measurement station on the Atlm University campus area in Ankara, Turkey. However, the Weibull distribution does not always consider the optimal alternative [14,22–25]. According to [14], a variety of mixture distributions, including the bimodal Weibull function (WW), truncated normal–Weibull function (NW), gamma–Weibull function (GW), and mixed truncated normal function (NN), outperformed the standard Weibull distribution.

Parametric distribution models can have one, two, three, or more parameters. Several estimation methods, such as the maximum likelihood method (MLM) [14,23,25], moment method (MM) [26], least square estimation (LSE) [14,27], empirical method (EM) [24,25], power density method (PDM) [25,28], and energy pattern factor (EPF) [26,29], should be used to properly estimate these parameters. Some modified methods have also been utilized, for example, the modified maximum likelihood method (MMLM) [26] and the modified energy pattern method (MEPM) [25].

In recent years, metaheuristic optimization approaches have been used to estimate the parameters of various distribution models. Some examples of such methods are particle swarm optimization (PSO) [27–30], cuckoo search optimization (CS) [14,29], genetic algorithm (GA) [26,28], differential evolution algorithm (DEA) [28], and grey wolf optimizer (GWO) [26]. The authors in [29] evaluated three optimization techniques, PSO, CS, and GWO, and compared them with four numerical methodologies. The performance of the algorithms was generally excellent, with GWO being the most precise technique. Saeed. et al. in [26] proposed artificial intelligence (AI)-based optimization techniques based on the Chebyshev measure for assessing wind potential at a site near Pakistan's coastline region. According to their findings, AI optimization outperformed numerical approaches by a factor of ten. In [27], a new metaheuristic optimization algorithm method called social spider optimization (SSO) was recommended for assessing wind potential in seven

areas in Saudi Arabia. According to the results, the proposed technique outperformed the other heuristic methods. However, several drawbacks limited the use of the parametric distribution models. One such drawback was the need for using estimating methods to determine the values of the parameters accurately. Therefore, some academics have suggested nonparametric distribution models. The most well-known method employed is the kernel density model (KDM) [5]. Normal scale (NS), plug-in, biased cross-validation, and least-square cross-validation were the four bandwidth selections presented by the authors of [5]. For comparisons with the KDE model, popular parametric distribution models were also introduced. The performance and resilience of both parametric and KDE models were examined exhaustively on a regional scale using five-year day-average wind speed data from 698 wind stations across China. Wind power density (WPD) and wind turbine power output (WTPO), which are the priorities in WEA, were then calculated based on the estimated PDWS models. The four KDE models outperformed the parametric models in fitting the PDWS, according to the results of four individual metrics. In comparison with the other three KDE models, the KDE–NS model performed the best.

The economic aspect is among the most important for the wind energy project [31–36]. Several shortcomings in the cost analysis of wind power projects have been identified in the literature. Some studies have used simplified cost-analysis models [35]. Such models are simple and easy to evaluate; however, they are free of detailed economic parameters and have a low accuracy level. Therefore, several research studies have used detailed economic models that are intrinsically about the time value of money [36–48]. Nevertheless, these models assume that the capital cost is constant for different energy production. In addition, the cost of the turbine system is not detailed for each component. Moreover, in these studies, the turbine selection process was not defined well but based on a trial-and-error procedure [15,23,36]. Alsaad, in [35], presented a study to assess wind energy resources in four selected sites in Jordan. The cost model adopted in this study was based on a net profit calculation. This model involved subtracting the total turbine cost from the total value of the energy sold, taking into account the salvage value throughout the operational period of the project. The weakness of this model is that it did not take into account the time value of money. This problem was avoided in [23,36]. The present value cost (PVC) model was used to calculate the cost of a wind turbine system. The limitation of this model is that the turbine price is specified as a particular USD/kWh rate multiplied by the turbine's rated power, and it is not adequately detailed. Therefore, the total cost of the turbine cannot be accurately predicted. Perkin et al., in [49], suggested an optimal approach for choosing wind turbine models in Iceland. This approach was based on utilizing the blade element theory and a detailed cost-analysis model. An optimization problem was established based on minimizing the cost of unit energy. The optimization variables were rotor length, rated power, hub height, pitch angle range, and rotations per minute. The same procedure was followed by the authors in [50], in which an optimal model was proposed to optimize the wind turbine parameters and achieve the minimum cost of unit energy for three sites in Iran.

This paper aims to fill the gap by providing a comprehensive study on the assessment of wind energy potential in Jordan. The study addressed the topic of wind energy estimation for wind turbine systems. Furthermore, the economic aspects of the wind systems installed at the selected wind sites were studied. This study addressed the previously identified shortcomings of cost analyses. It also presented an optimal cost analysis intended to minimize the cost of unit energy using the whale optimization algorithm (WOA). In addition, the detailed turbine cost model developed by the U.S. National Renewable Energy Laboratory (NREL) is discussed and was used in this study [51].

The rest of the paper is organized as follows: Section 2 describes the evolution of wind energy in Jordan; the energy extracted from wind turbines is presented in Section 3; cost analysis of the designed systems is presented in Sections 4 and 5; the optimization problem is defined in Section 6; extrapolation method of wind speed is illustrated in Section 7;

results and discussion are presented in Section 8; real measurements and the validation process are discussed in Section 9; and conclusions are presented in Section 10.

2. Evolution of Wind Energy in Jordan

In 1988, the city of Al-Ibrahimia built Jordan's first wind farm. It consists of four 320 kW wind turbines. In 1996, in Hofa, Jordan, the second wind farm was established. It has a total capacity of 1.125 Mw and is made up of five wind turbines. Two new wind farms have recently been built. The first is in Tafila province, with 38 turbines rated at 3.075 MW apiece and a total capacity of 117 Mw. The second wind farm is in Ma'an, with seven turbines rated at two MW each and a total capacity of 14 MW.

The evolution of Jordan's wind energy capacity is depicted in Figure 1. Wind farms that were operational in 2017 produced 132 MW of energy. Wind farms with a capacity of 155 MW are now being built and will be connected to the grid soon [43]. Table 1 provides additional information on Jordanian wind farms that have been operated or were currently under development between 1988 and 2017.

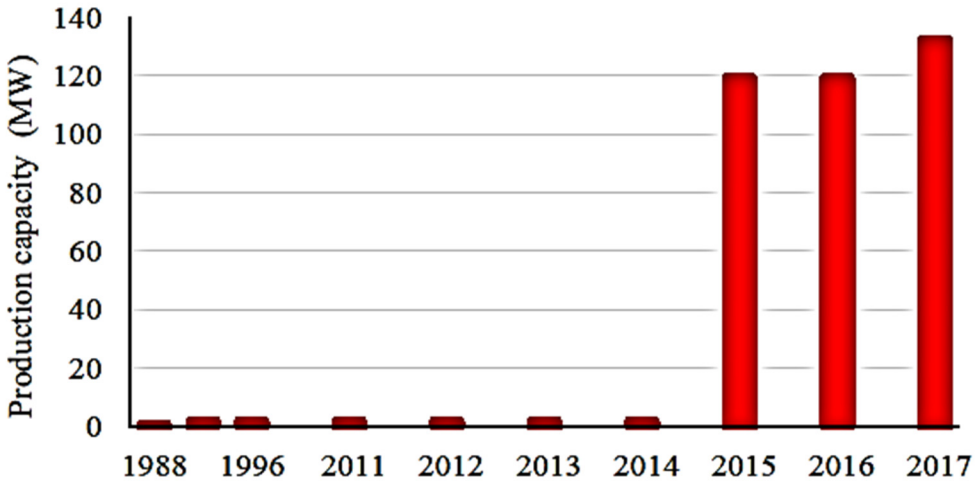

Figure 1. The evolution of the wind production capacity in Jordan.

Table 1. Distribution of wind farms in Jordan.

Project	Number of Turbines	Turbine Model	Turbine Rated Power (kW)	V_I (m/s)	V_R (m/s)	V_o (m/s)	Hub Height (m)	Total Capacity (MW)
Tafila	38	Vestas V112/3075	3075	2.5	13	25	84	116.85
Hofa	5	Vestas V27/225	2250	3.5	14	22	33.5	1.125
Fujeij	27	Gamesa G126/3300	3300	2.5	12	25	117	89.1
Al Rajef	41	Gamesa G114/2000	2000	3	11	25	80	86.1
Daehan	15	Vestas V136/3450	3450	2.5	11	22	149	51.75

3. Energy Extracted from Different Wind Turbine Models

The power of the wind passing through the wind turbine P_T can be expressed as follows [52–54]:

$$P_T = \frac{1}{2}\rho_a A\, v^3 \quad (1)$$

where ρ_a is the air density in (kg/m^3), A is the rotor swept area in (m^2) and v is the wind speed (m/s). The output power generated by the wind turbine can be given in terms of the turbine power coefficient (C_p), as follows [55]:

$$P = \frac{1}{2}\rho_a A C_p \eta_m \eta_g v^3 \tag{2}$$

where C_p is the blade aerodynamic efficiency factor, η_m and η_g are gearbox and generator efficiencies, respectively. These factors are given by the manufacturer depending on blade design, blade shape and type of wind turbine [47].

Each wind turbine has its own Power–Velocity (P–V) curve, which consists of two performance regions: performance region 1 (non-linear region) and performance region 2 (constant region). Figure 2 shows the P–V curve of a typical turbine model and its performance regions. The non-linear region is expressed using several mathematical expressions in terms of rated power (P_v) cut-in speed (v_i), rated speed (v_r), and cut-out speed (v_o) [29].

$$P(v) = \begin{cases} 0, & v < v_i \ \ or \ \ v > v_o \\ Q(v), & v_i \le v < v_r \quad (Performance\ region\ 1) \\ P_R, & v_r \le v \le v_o \quad (Performance\ region\ 2) \end{cases} \tag{3}$$

where $Q(v)$ represents the mathematical expression of the non-linear region of the P–V curve, which can be linear, quadratic, cubic, or exponential [9,56]. The linear expression shows several deficiencies and less accuracy according to [56]. Therefore, in this paper five different expressions, excluding the linear model, are used to represent the non-linear region of the turbine model [56]:

$$Q_1(v) = P_R\left(\frac{v^2 - v_i^2}{v_r^2 - v_i^2}\right) \tag{4}$$

$$Q_2(v) = P_R\left(a_1 + a_2 v + a_3 v^2\right) \tag{5}$$

$$Q_3(v) = P_R\left(1 - e^{-\left(\frac{v}{\alpha}\right)^5}\right) \tag{6}$$

$$Q_4(v) = P_R\left(\frac{v^3}{v_r^3}\right) \tag{7}$$

$$Q_5(v) = P_R\left(\frac{v^3 - v_i^3}{v_r^3 - v_i^3}\right) \tag{8}$$

where α is a constant value in terms of rated speed (v_r), $\alpha = 0.70335986 v_r - 0.00049995$.

And:

$$a_1 = v_i\left(v_a - 2v_r\left(\frac{v_a}{v_r}\right)^3\right)\frac{0.5}{(v_r - v_a)^2} \tag{9}$$

$$a_2 = \left(v_r - 3v_a + 4v_a\left(\frac{v_a}{v_r}\right)^3\right)\frac{0.5}{(v_r - v_a)^2} \tag{10}$$

$$a_3 = \left(1 - 2\left(\frac{v_a}{v_r}\right)^3\right)\frac{0.5}{(v_r - v_a)^2} \tag{11}$$

$$v_a = \frac{1}{2}(v_i + v_r) \tag{12}$$

Therefore, the energy produced by the wind turbine in both performance regions can be calculated as follows [3]:

$$E_{ir} = T \int_{v_i}^{v_r} Q(v)\, f(v)\ dv \tag{13}$$

$$E_{ro} = TP_R \int_{v_r}^{v_o} f(v)\ dv \tag{14}$$

$$E_{Total} = (1 - \mu)(E_{ir} + E_{ro}) \tag{15}$$

where T is the number of hours in a specific period, E_{ir} is the energy produced by the wind turbine in performance region one in *MWh*. E_{ro} is the energy produced by the wind turbine in performance region two in *MWh*, E_{total} is the total energy produced by the wind turbine in the two performance regions in *MWh* and μ is the total turbine losses, which comprise power converter losses, electrical grid losses, and soiling losses, in addition to some losses that are related to the turbine design and wind distribution [57].

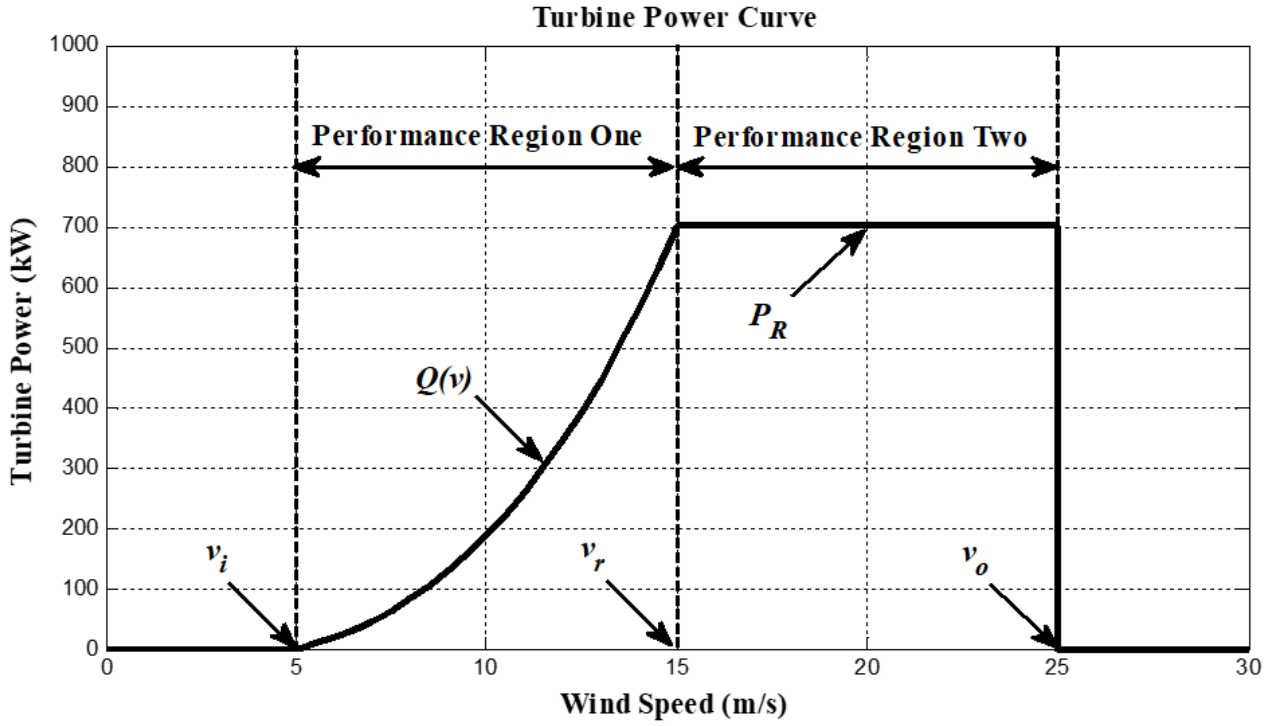

Figure 2. Typical Power-Speed model of wind turbine.

The ability of the wind turbine to produce electricity can be examined by the definition of the capacity factor (*CF*). This factor is the major indicator to choosing a proper wind turbine in a specific wind site and it can be expressed as follows [52].

$$CF = \frac{E_{Total}}{T \times P_R} \tag{16}$$

In this paper, using the power curve model presented by (4)–(8), the total energy extracted by the wind turbine (E_{Total}) is derived based on Weibull and Gamma distribution functions. This will be presented in the following subsections.

3.1. Energy Extracted by Q1(v) Based on Weibull Distribution

The distribution function of Weibull model is expressed as follows [57]:

$$f_w(v) = \frac{k}{c}\left(\frac{v}{c}\right)^{k-1} e^{-(v/c)^k} \tag{17}$$

where k and c refer to shape and scale parameters, respectively. Substitute (4) and (17) in (15) and simplify, yields:

$$\begin{aligned} E_{Q1_w} = \tfrac{T\ P_R}{v_r^2 - v_i^2}\Big(c^2\Big(\Gamma\Big(\tfrac{k+2}{k}, \big(\tfrac{v_i}{c}\big)^k\Big) - \Gamma\Big(\tfrac{k+2}{k}, \big(\tfrac{v_r}{c}\big)^k\Big)\Big) \\ - v_i^2\Big(e^{-\left(\frac{v_i}{c}\right)^k} - e^{-\left(\frac{v_r}{c}\right)^k}\Big)\Big) + TP_R\Big(e^{-\left(\frac{v_r}{c}\right)^k} - e^{-\left(\frac{v_o}{c}\right)^k}\Big) \end{aligned} \tag{18}$$

where $\Gamma(a, x)$ is the upper incomplete gamma function.

3.2. Energy Extracted by $Q_1(v)$ Based on Gamma Distribution

The distribution function of Gamma model is expressed as follows [57].

$$f_G(v) = \left(\frac{v}{c}\right)^k \frac{e^{-(v/c)}}{\Gamma(k)\, v} \tag{19}$$

where Γ is the gamma function. Substitute (4) and (19) in (15) and simplify, yields:

$$\begin{aligned} E_{Total} = \tfrac{T\ P_R}{\Gamma(k)\left(v_r^2 - v_i^2\right)}\left(c^2\left(\Gamma\left(k+2\,,\ \tfrac{v_i}{c}\right) - \Gamma\left(k+2\,,\ \tfrac{v_r}{c}\right)\right)\right. \\ \left. - v_i^2\left(\Gamma\left(k\,,\ \tfrac{v_i}{c}\right) - \Gamma\left(k\,,\ \tfrac{v_r}{c}\right)\right)\right) + \tfrac{T\ P_R}{\Gamma(k)}\left(\Gamma\left(k\,,\ \tfrac{v_r}{c}\right) - \Gamma\left(k\,,\ \tfrac{v_o}{c}\right)\right) \end{aligned} \tag{20}$$

3.3. Energy Extracted by $Q_2(v)$ Based on Weibull and Gamma Distribution

Similarly, the total energy extracted by $Q_2(v)$ has been calculated for each distribution model. Substitute (5) and (17) in (15) and simplify, yields:

$$\begin{aligned} E_{Q2_w} = T\ P_R\Big[a_1\left(e^{-\left(\frac{v_i}{c}\right)^k} - e^{-\left(\frac{v_r}{c}\right)^k}\right) \\ + a_2 c\Big(\Gamma\Big(\tfrac{k+1}{k}, \big(\tfrac{v_i}{c}\big)^k\Big) - \Gamma\Big(\tfrac{k+1}{k}, \big(\tfrac{v_r}{c}\big)^k\Big)\Big) \\ + a_3 c^2\Big(\Gamma\Big(\tfrac{k+2}{k}, \big(\tfrac{v_i}{c}\big)^k\Big) - \Gamma\Big(\tfrac{k+2}{k}, \big(\tfrac{v_r}{c}\big)^k\Big)\Big) \\ + \Big(e^{-\left(\frac{v_r}{c}\right)^k} - e^{-\left(\frac{v_o}{c}\right)^k}\Big)\Big] \end{aligned} \tag{21}$$

where E_{Q2_w} is the total energy extracted by the turbine model Q_2 and Weibull distribution. Additionally, substitute (5) and (19) in (15) and simplify to find E_{Q2_G}:

$$\begin{aligned} E_{Q2_G} = \tfrac{T\ P_R}{\Gamma(k)}\left[a_1\left(\Gamma\left(k\,,\ \tfrac{v_i}{c}\right) - \Gamma\left(k\,,\ \tfrac{v_r}{c}\right)\right) + a_2 c\left(\Gamma\left(k+1\,,\ \tfrac{v_i}{c}\right) - \Gamma\left(k+1\,,\ \tfrac{v_r}{c}\right)\right)\right. \\ + a_3 c^2\left(\Gamma\left(k+2\,,\ \tfrac{v_i}{c}\right) - \Gamma\left(k+2\,,\ \tfrac{v_r}{c}\right)\right) \\ \left. + \left(\Gamma\left(k\,,\ \tfrac{v_r}{c}\right) - \Gamma\left(k\,,\ \tfrac{v_o}{c}\right)\right)\right] \end{aligned} \tag{22}$$

where E_{Q2_G} is the total energy extracted by the turbine model Q_2 and Gamma distribution.

3.4. Energy Extracted by $Q_3(v)$ Based on Weibull and Gamma Distribution

The total energy extracted by the exponential power curve $Q_3(v)$ has been calculated for each distribution model. Substitute (6) and (17) in (15) and simplify, yields:

$$E_{Q3_w} = T\ P_R\left(e^{-(\frac{v_r}{c})^k} - e^{-(\frac{v_o}{c})^k} - \int_{v_i}^{v_r} \frac{k}{c^k} v^{k-1} e^{-(v/c)^k-(v/a)^5} dv\right) \tag{23}$$

where E_{Q2_w} is the total energy extracted by the turbine model Q_2 and Weibull distribution. Additionally, substitute (6) and (19) in (15) and simplify to find E_{Q3_G}:

$$E_{Q3_G} = \frac{T\ P_R}{\Gamma(k)}\left(\Gamma\left(k\ ,\ \frac{v_i}{c}\right) - \Gamma\left(k\ ,\ \frac{v_o}{c}\right) - \int_{v_i}^{v_r} \frac{v^{k-1}}{c^k} e^{-(v/c)^k-(v/a)^5} dv\right) \tag{24}$$

where E_{Q3_G} is the total energy extracted by the turbine model Q_3 and Gamma distribution.

3.5. Energy Extracted by $Q_4(v)$ Based on Weibull and Gamma Distribution

The total energy produced by the cubic power curve $Q_4(v)$ has been calculated for each distribution model. Substitute (7) and (17) in (15) and simplify, yields:

$$\begin{aligned} E_{Q4_w} = T\ P_R \frac{c^3}{v_r^3}\left(\Gamma\left(\tfrac{k+3}{k}, \left(\tfrac{v_i}{c}\right)^k\right) - \Gamma\left(\tfrac{k+3}{k}, \left(\tfrac{v_r}{c}\right)^k\right)\right) \\ +T\ P_R\left(e^{-(\frac{v_r}{c})^k} - e^{-(\frac{v_o}{c})^k}\right) \end{aligned} \tag{25}$$

where E_{Q4_w} is the total energy extracted by the turbine model Q_4 and Weibull distribution. Additionally, substitute (7) and (19) in (15) and simplify to find E_{Q4_G}:

$$E_{Q3_w} = \frac{T\ P_R}{\Gamma(k)} \frac{c^3}{v_r^3}\left(\Gamma\left(k+3\ ,\ \frac{v_i}{c}\right) - \Gamma\left(k+3\ ,\ \frac{v_r}{c}\right)\right) + \frac{T\ P_R}{\Gamma(k)}\left(\Gamma\left(k\ ,\ \frac{v_r}{c}\right) - \Gamma\left(k\ ,\ \frac{v_o}{c}\right)\right) \tag{26}$$

where E_{Q4_G} is the total energy extracted by the turbine model Q_4 and Gamma distribution.

3.6. Energy Extracted by $Q_5(v)$ Based on Weibull and Gamma Distribution

Finally, the total energy produced by $Q_5(v)$ has been calculated for each distribution model. Substitute (8) and (17) in (15) and simplify, yields:

$$\begin{aligned} E_{Q5_w} = TP_R\left(\frac{c^3}{v_r^3 - v_i^3}\left(\Gamma\left(\tfrac{k+3}{k}, \left(\tfrac{v_i}{c}\right)^k\right) - \Gamma\left(\tfrac{k+3}{k}, \left(\tfrac{v_r}{c}\right)^k\right)\right)\right. \\ \left. -\frac{v_i^3}{v_r^3 - v_i^3}\left(e^{-(\frac{v_i}{c})^k} - e^{-(\frac{v_r}{c})^k}\right) + \left(e^{-(\frac{v_r}{c})^k} - e^{-(\frac{v_o}{c})^k}\right)\right) \end{aligned} \tag{27}$$

where E_{Q5_w} is the total energy extracted by the turbine model Q_5 and Weibull distribution. Additionally, substitute (8) and (19) in (15) and simplify to find E_{Q5_G}:

$$\begin{aligned} E_{Q5_G} = \frac{TP_R}{\Gamma(k)}\left(\frac{c^3}{v_r^3 - v_i^3}\left(\Gamma\left(k+3\ ,\ \tfrac{v_i}{c}\right) - \Gamma\left(k+3\ ,\ \tfrac{v_r}{c}\right)\right)\right. \\ \left. -\frac{v_i^3}{v_r^3 - v_i^3}\left(\Gamma\left(k\ ,\ \tfrac{v_i}{c}\right) - \Gamma\left(k\ ,\ \tfrac{v_r}{c}\right)\right) + \left(\Gamma\left(k\ ,\ \tfrac{v_r}{c}\right) - \Gamma\left(k\ ,\ \tfrac{v_o}{c}\right)\right)\right) \end{aligned} \tag{28}$$

where E_{Q5_G} is the total energy extracted by the turbine model Q_5 and Gamma distribution.

4. Cost Analysis

The Net Present Value CostNPV_C method, which can be mathematically presented as in [51], is used to perform the cost analysis in this study.

$$NPV_C = P_d + P_a Y\left(\frac{1}{1+b}, N\right) + C_c f_{OM} Y\left(\frac{1+i}{1+r}, L\right) \tag{29}$$

where,

$$P_a{=}(C_C - P_d)\, CRF \tag{30}$$

Additionally, P_a and P_d are the annual and down payments on system cost, respectively. C_c is the capital cost of the system. and P_d is the down payment on system cost. CRF is the capital recovery factor, based on the loan interest rate(b), rather than the discount rate (r). i is the inflation rate in (%), N is the loan period, L is the system lifetime, f_{oM} is the annual operating and maintenance cost (fraction of the capital cost) and $Y(K, l)$is a function used to obtain the present value of a series of payments which can be evaluated by (31):

$$Y(K,l) = \sum_{j=1}^{l} K^j = \begin{cases} \frac{K-K^{l+1}}{1-K}, & K \neq 1 \\ l, & K = 1 \end{cases} \tag{31}$$

For simplifications and research purposes, it is assumed that P_d and b are equal to zero. By applying (31) and considering the previous assumptions, (29) can be rewritten as follows:

$$NPV_C = C_c\left(1 + f_{OM}\left[\frac{(1+i) - (1+i)^{1+L}(1+r)^{-L}}{r-i}\right]\right) \tag{32}$$

Accordingly, the Levelized cost of energy ($LCoE$) can be expressed as follows [51]:

$$LCoE = \frac{NPV_C \times CRF}{E_{Total}} \tag{33}$$

where CRF can be expressed as follows [47]:

$$CRF = \begin{cases} \frac{r}{1-(1+r)^{-L}}, & r \neq 0 \\ \frac{1}{L}, & r = 0 \end{cases} \tag{34}$$

5. Capital Cost Model and Its Correction Factor

The capital cost model can be divided into four main parts: (a) turbine system cost, (b) network connection cost, (c) civil work cost, and (d) other costs, including engineering permits, consultancy, transactions, and monitoring systems [46,58–62].

The original capital cost model which was developed by the National Renewable Energy Laboratory (NREL) has been evaluated based on the value of the US dollar in 2002 [51]. Therefore, in this study, the resultant capital cost of this model is corrected by a factor of 1.6. This correction factor was used to consider the difference in currency value between the 2002 cost model (NREL cost model) and the value of currency during the periods at which the wind projects were built. It has been calculated as follows: the actual turbine cost for each project, which is given by several sources [63–75], was divided by the turbine cost and evaluated based on the NREL model to find the individual correction factor for each project. Then, an average value of the correction factors for all projects was calculated, as illustrated in Table 2.

Table 2. Method of scaling factor calculation.

Project Name	Turbine Model	Number of Turbines	Overall Real Cost (Million $)	Real Cost per Turbine (Million $)	Model Cost per Turbine (Million $)	Scaling Factor
Jordan Wind—Tafileh [63,75]	Vestas(V112/3.075) 84m HH	4	287 (10.53%) 30.2211	7.555275	3.687782	2.0487
	Vestas(V112/3.075) 94m HH	34	(89.47%) 256.7789	7.552321	3.762716	2.0071
AlRajef [64,65,75]	Gamesa(114/2.100) 80m HH	41	184.6	4.502439	3.087002	1.4585
Deahan [66–68,75]	Vestas(V136/3.450) 112m HH	15	102	6.800000	5.411168	1.2567
Shobak [69,75]	Vestas(V136/3.450) 112m HH	13	104	8.000000	5.411168	1.4784
Fujejji [70,71,75]	Vestas(V126/3.300) 117m HH	27	180	6.666667	4.785160	1.3932
Al-Hussein University [72–75]	Gamesa(97/2.000) 78m HH	40	148	3.700000	2.407814	1.5367
Average Scaling Factor						1.5970 ≈ 1.6

6. Optimization Problem

In this study, nine wind sites in Jordan were selected for wind farms installation purposes. These wind sites are Queen Alia Airport, Amman Civil Airport, King Hussein Airport, Irbid, Mafraq, Ma'an, Safawi, Irwaished, and Ghor Es Safi. They have been selected based on two main factors: the first one is the geographical distribution which allows us to carry out a comprehensive study that includes various regions in Jordan (from north, south, east, west, and center). The second factor is the average wind speed in these wind sites, which is considered to be strong and can potentially be compared with other wind sites. A map showing the locations of these wind sites in Jordan is presented in Figure 3. Based on the Global Wind Energy Atlas (GWEA), the recorded wind speed is the highest in these wind sites, as illustrated in Table 3. Therefore, in our study wind turbines with specific features are suggested for the proposed wind farms to obtain maximum extracted energy, maximum *CF,* and minimum *LCoE.* To solve the developed optimization problem, a whale optimization algorithm is used to obtain the desired objective functions for the selected wind sites.

Table 3. The location and the average wind speed of the selected wind site at 100 m height.

Wind Site	Longitude and Latitude	Average Wind Speed (m/s)
Queen Alia Airport	35°59′21.59″ E, 31°43′12.59″ N	7.25
Amman Civil Airport	35°59′17.39″ E, 31°58′12.59″ N	6.7
King Hussein Airport	35°01′3.02″ E, 29°36′25.09″ N	5.93
Irbid	35°51′25.751″ E, 32°32′43.591″ N	6.58
Mafraq	36°11′60.00″ E, 32°20′59.99″ N	7.63
Ma'an	35°44′3.2676″ E, 30°11′41.8488″ N	8.11
Safawi	37°126′2763″ E, 32°19′2941″ N	7.1
Irwaished	38°7′26″ E, 32°18′5″ N	6.1
Ghor Es Safi	35°27′55.58″ E, 31°02′9.89″ N	5.8

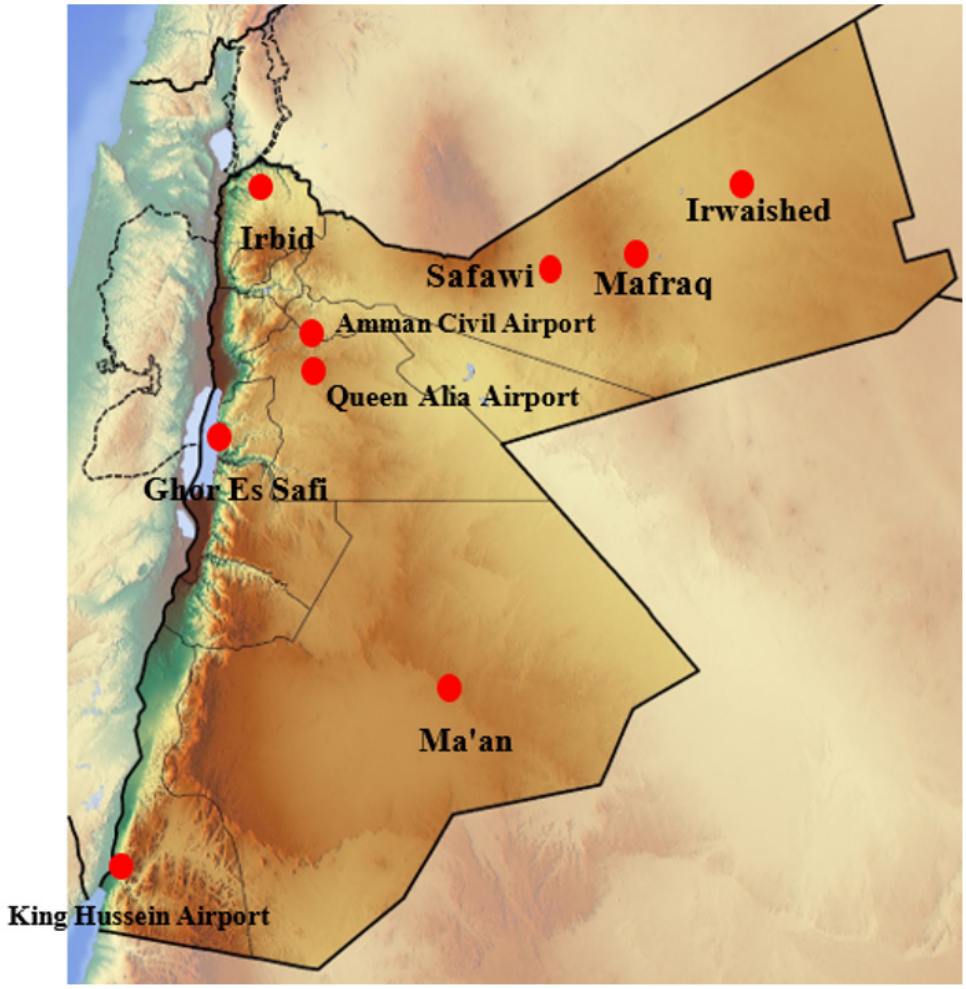

Figure 3. The location of the wind sites under test in Jordan Map.

According to (37), there are six optimization variables in the Levelized Cost of Energy (*LCoE*) equation which are $(P_R,\ R,\ H,\ v_i,\ v_r,\ and\ v_o)$. The number of variables can be reduced to only two optimization variables $(P_R,\ v_r)$ by making some manipulations and assumptions which can be summarized in the following points:

By rearranging (2), the rotor radius can be represented in terms of rated power and rated speed, as expressed in (35):

$$R = \sqrt{\frac{2P_R}{\rho_a \pi C_p \eta_m \eta_g v_r^3}} \tag{35}$$

The hub height can be expressed as a function of the rotor radius by the following empirical formula, according to European Wind Energy Association (EWEA) [76–80]:

$$H = 2.7936 \times (2R)^{0.7663} \tag{36}$$

Most of the commercial wind turbines have cut-in speed in the range of 3–4 m/s (assumed v_i = 3.5 m/s), and a cut-out speed of 25 m/s.

By considering the previous points and assumptions, the *LCoE* can be simplified in terms of rated power and rated speed, as follows:

$$LCoE = f(P_R,\ v_r) \tag{37}$$

The entire steps of the optimization problem are summarized in a flowchart illustrated in Figure 4.

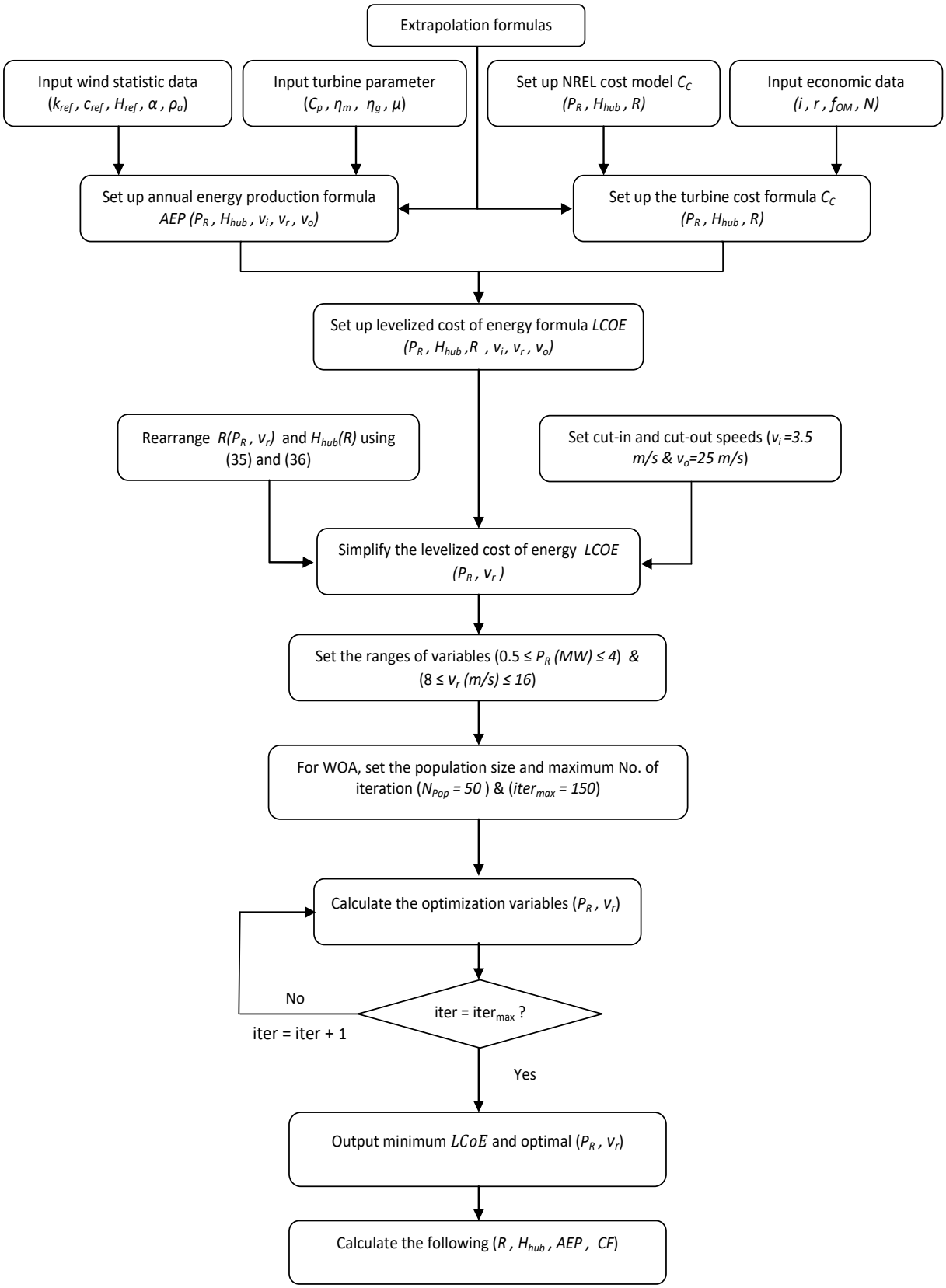

Figure 4. The flowchart of the optimization problem.

7. Extrapolation of Wind Speed at Different Height

Wind speed is varying with height by a power-law expressed as follows [77,78]:

$$v = v_{ref}\left(\frac{H}{H_{ref}}\right)^{\alpha} \tag{38}$$

where v_{ref} is the wind speed at reference height H_{ref}, is the wind speed at the hub height H. The factor α represents the wind shear exponent. Accordingly, the shape and scale factors can be calculated at the hub height H for different distribution models.

8. Results and Discussion

The utilized algorithms were implemented in MATLAB R2007 b, with the following specifications: Intel® core (TM) i3-2330 M CPU @ 2.20 GHz, Installed memory (RAM): 4.00 GB, System type: 64-bit Operating system. The optimization process considered a stopping criterion of 150 iterations and a population size of 50 for each algorithm. The statistical information for each site is presented in Table 4. The wind shear exponent (α) determined for each site according to different terrain types is also presented in Table 4, except for the King Hussein site, in which the shear exponent factor is evaluated using (77). These data are used as input for our optimization problem. Furthermore, the detailed parameters of the *LCoE* model are provided in Table 5. The rated power P_R and rated speed v_r have ranges of (0.5–4) *MW* and (8–16) m/s, respectively.

Table 4. The statistical data for the selected sites.

Wind Site	Shape Factor k_{ref}	Scale Factor $c_{ref}(m/s)$	Reference Height $H_{ref}(m)$	Shear Exponent A
Queen Alia Airport	4.02	1.17	10	0.15
Amman Civil Airport	3.48	1.15	10	0.15
King Hussein Airport	2.78	5.93	10	0.21
Irbid	7.33	0.30	10	0.25
Mafraq	5.33	0.71	10	0.15
Ma'an	8.62	0.46	10	0.15
Safawi	6.50	0.76	10	0.15
Irwaished	4.52	0.91	10	0.15
Ghor Es Safi	6.71	0.36	10	0.20

Table 5. The levelized cost of energy parameters.

Parameter	Value
No. of blades	3
Air density (ρ_a)	1.225 Kg/m^3
Blade aerodynamic efficiency (C_P)	0.45 [9,78]
Gearbox efficiency (η_m)	0.96 [78]
Generator efficiency (η_g)	0.97 [78]
Total turbine losses (μ)	0.15 [51]
Cut–in speed (v_i)	3.5 m/s
Cut–out speed (v_o)	25 m/s
Discount rate (r)	2.5% [79]
Inflation rate (i)	0.3% [80]
O & M percentage (f_{OM})	3.5% [3]
Lifetime of system (L)	20 year [3,51]

Table 6. provides the optimal values of the objective function for each site, which are obtained by the utilized optimization algorithm. A closer inspection of this table shows that the ranges of the rotors' lengths and hubs' heights are between (37–45 m) and (77–88 m), respectively. The annual energy production, capacity factor, and the minimum cost of

energy for all sites are summarized in Table 7. It is clear from the results obtained in this table that the exponential power model $Q_3(v)$ shows a clear superiority over the other power models in calculating the capacity factor and *LCoE*. Accordingly, King Hussein Airport achieves the best results among other sites by recording the minimum *LCoE* and maximum *CF*, 33.81 *$/MWh* and 0.54, respectively. The higher *LCoE* are recorded by Ghor Es Safi with a value of around (405.00 *$/MWh*) and a *CF* value of around 0.11.

Table 6. The optimal values of the optimization variables.

Site	**Queen Alia Airport**					**Amman Civil Airport**				
Model	$Q_1(v)$	$Q_2(v)$	$Q_3(v)$	$Q_4(v)$	$Q_5(v)$	$Q_1(v)$	$Q_2(v)$	$Q_3(v)$	$Q_4(v)$	$Q_5(v)$
k	4.02	4.02	4.02	4.02	4.02	3.48	3.48	3.48	3.48	3.48
c (m/s)	1.6	1.6	1.59	1.59	1.6	1.58	1.57	1.57	1.57	1.58
Vr (m/s)	10.59	9.63	10.25	9.7	9.72	10.21	9.12	9.69	9.22	9.26
Pr (MW)	1.48	1.13	1.25	1.12	1.21	1.46	1	1.12	1	1.11
R (m)	39.33	39.54	37.96	39.02	40.32	41.21	40.47	39.04	39.84	41.64
H (m)	79.22	79.55	77.1	78.76	80.75	82.12	80.99	78.78	80.02	82.76
Site	**King Hussein Airport**					**Irbid**				
Model	$Q_1(v)$	$Q_2(v)$	$Q_3(v)$	$Q_4(v)$	$Q_5(v)$	$Q_1(v)$	$Q_2(v)$	$Q_3(v)$	$Q_4(v)$	$Q_5(v)$
k	3.42	3.43	3.4	3.43	3.43	7.33	7.33	7.33	7.33	7.33
c (m/s)	9.33	9.39	9.24	9.38	9.42	0.58	0.58	0.57	0.57	0.59
Vr (m/s)	10.77	10.22	11.1	10.21	10.18	8	8	8	8	8
Pr (MW)	1.8	1.67	1.75	1.64	1.7	2.72	2.85	2.15	2.4	3.07
R (m)	42.26	44.01	39.85	43.75	44.66	81.16	83.04	72.16	76.17	86.2
H (m)	83.72	86.35	80.03	85.96	87.34	138.03	140.48	126.14	131.48	144.56
Site	**Mafraq**					**Ma'an**				
Model	$Q_1(v)$	$Q_2(v)$	$Q_3(v)$	$Q_4(v)$	$Q_5(v)$	$Q_1(v)$	$Q_2(v)$	$Q_3(v)$	$Q_4(v)$	$Q_5(v)$
k	5.33	5.33	5.33	5.33	5.33	8.62	8.62	8.62	8.62	8.62
c (m/s)	0.98	0.97	0.97	0.97	0.98	0.63	0.63	0.62	0.62	0.63
Vr (m/s)	9.42	8.19	8.84	8.31	8.3	8.92	8	8.48	8	8
Pr (MW)	1.34	0.75	0.88	0.75	0.85	1.2	0.75	0.77	0.68	0.82
R (m)	44.56	41.13	39.85	40.22	43.05	45.8	42.72	39.65	40.69	44.64
H (m)	87.19	81.99	80.02	80.59	84.91	89.03	84.41	79.73	81.31	87.3
Site	**Safawi**					**Irwaished**				
Model	$Q_1(v)$	$Q_2(v)$	$Q_3(v)$	$Q_4(v)$	$Q_5(v)$	$Q_1(v)$	$Q_2(v)$	$Q_3(v)$	$Q_4(v)$	$Q_5(v)$
k	6.5	6.5	6.5	6.5	6.5	4.52	4.52	4.52	4.52	4.52
c (m/s)	1.04	1.04	1.03	1.04	1.04	1.25	1.24	1.24	1.24	1.24
Vr (m/s)	10.18	9.23	9.98	9.29	9.28	9.92	8.81	9.44	8.91	8.92
Pr (MW)	1.4	1.01	1.18	1	1.08	1.4	0.91	1.05	0.91	1.01
R (m)	40.52	39.85	38.4	39.26	40.91	42.23	40.65	39.33	39.94	42.08
H (m)	81.06	80.03	77.78	79.12	81.66	83.67	81.26	79.23	80.17	83.44

Table 6. *Cont.*

Site	**Ghor Es Safi**				
Model	$Q_1(v)$	$Q_2(v)$	$Q_3(v)$	$Q_4(v)$	$Q_5(v)$
k	6.7	6.7	6.7	6.7	6.7
c (m/s)	0.59	0.59	0.58	0.59	0.6
Vr (m/s)	8.04	8	8	8	8
Pr (MW)	2.1	2.17	1.62	1.77	2.35
R (m)	70.68	72.54	62.6	65.5	75.51
H (m)	124.15	126.65	113.13	117.12	130.61

Table 7. *AEP*, *CF*, and *LCoE* results.

Site	**Queen Alia Airport**					**Amman Civil Airport**				
Model	$Q_1(v)$	$Q_2(v)$	$Q_3(v)$	$Q_4(v)$	$Q_5(v)$	$Q_1(v)$	$Q_2(v)$	$Q_3(v)$	$Q_4(v)$	$Q_5(v)$
AEP (MWh)	3721.85	3000.81	3949.3	3011.24	3041.65	2852.56	2157.12	2918.06	2184.02	2215.87
CF	0.29	0.3	0.36	0.31	0.29	0.22	0.25	0.3	0.25	0.23
LCoE ($/MWh)	67.9	75.2	56.56	73.45	78.39	93.47	103.65	75.75	100.01	109.24
Site	**King Hussein Airport**					**Irbid**				
Model	$Q_1(v)$	$Q_2(v)$	$Q_3(v)$	$Q_4(v)$	$Q_5(v)$	$Q_1(v)$	$Q_2(v)$	$Q_3(v)$	$Q_4(v)$	$Q_5(v)$
AEP (MWh)	7573.1	7169.74	8275.35	7061.56	7168.75	3755.52	3719.72	4341.78	3320.47	3611.04
CF	0.48	0.49	0.54	0.49	0.48	0.16	0.15	0.23	0.16	0.13
LCoE ($/MWh)	40.2	43.21	33.81	43.22	44.47	287.6	308.61	183.22	275.48	351.42
Site	**Mafraq**					**Ma'an**				
Model	$Q_1(v)$	$Q_2(v)$	$Q_3(v)$	$Q_4(v)$	$Q_5(v)$	$Q_1(v)$	$Q_2(v)$	$Q_3(v)$	$Q_4(v)$	$Q_5(v)$
AEP (MWh)	2571.06	1716.58	2472.59	1729.12	1784.36	2718.95	1969.03	2583.55	1837.73	1993.79
CF	0.22	0.26	0.32	0.26	0.24	0.26	0.3	0.38	0.31	0.28
LCoE ($/MWh)	111.92	121.7	84.48	116.32	131.45	106.37	113.5	76.84	108.79	124.1
Site	**Safawi**					**Irwaished**				
Model	$Q_1(v)$	$Q_2(v)$	$Q_3(v)$	$Q_4(v)$	$Q_5(v)$	$Q_1(v)$	$Q_2(v)$	$Q_3(v)$	$Q_4(v)$	$Q_5(v)$
AEP (MWh)	4110.25	3207.76	4387.37	3181.22	3261.82	2969.41	2164.48	3007.72	2179.65	2233.72
CF	0.34	0.36	0.42	0.36	0.35	0.24	0.27	0.33	0.27	0.25
LCoE ($/MWh)	62.17	68.16	50.38	66.98	71.52	91.34	100.61	72.41	97.11	106.77
Site	**Ghor Es Safi**									
Model	$Q_1(v)$		$Q_2(v)$		$Q_3(v)$	$Q_4(v)$			$Q_5(v)$	
AEP (MWh)	2317.23		2286.6		2728.66	2021.04			2208.2	
CF	0.13		0.12		0.19	0.13			0.11	
LCoE ($/MWh)	327.02		352.68		203.93	308.11			405	

Table 8 provides a comparison between the results obtained in this study and those presented in [41]. Ammari at el. in [41] presented an assessment study of the wind energy potential of five wind sites in Jordan. The Weibull distribution model and five commercial wind turbines were utilized to calculate the Annual Energy Produced (AEP) and the corresponding *CF* in each site. The common wind sites between our study and the study in [41] are compared with each other in terms of *AEP* and CF. These wind sites are Queen Alia Airport, King Hussein Airport (Aqaba), and Safawi. To conduct a comparative

analysis, the developed optimal approach in our model has been applied to the same turbine models used in the study of [41]. Table 8 shows the comparison between the results obtained by the two studies. A closer inspection of this table shows that the results of our study are superior to those obtained by [41] for most wind turbines. The presented results are significant and confirm that our proposed approach is recommended to be applied for wind energy estimation.

Table 8. Comparison between the results of the proposed study and the results presented in [41].

Model Type	**Fuhrlander-100**					
Study	**Our Proposed Model**			**Study in Ref. [41]**		
Site	Q. A. Airport	K. H. Airport	Safawi	Q. A. Airport	K. H. Airport	Safawi
AEP (MWh)	147.97	235.11	148.79	60.42	313.45	147.42
CF (%)	16.9	26.8	17	6.8	35.7	16.8
Model Type	**EWT-500**					
Study	**Our Proposed Model**			**Study in Ref. [41]**		
Site	Q. A. Airport	K. H. Airport	Safawi	Q. A. Airport	K. H. Airport	Safawi
AEP (MWh)	1390.16	2178.04	1530.07	556.6	2086.32	1257.11
CF (%)	31.7	49.7	34.9	12.7	47.6	28.7
Model Type	**EWT-900**					
Study	**Our Proposed Model**			**Study in Ref. [41]**		
Site	Q. A. Airport	K. H. Airport	Safawi	Q. A. Airport	K. H. Airport	Safawi
AEP (MWh)	1403.23	2283.77	1422.53	582.94	2448.36	1379.99
CF (%)	17.8	29	18	7.3	31.1	17.5
Model Type	**Fuhrlander-1500**					
Study	**Our Proposed Model**			**Study in Ref. [41]**		
Site	Q. A. Airport	K. H. Airport	Safawi	Q. A. Airport	K. H. Airport	Safawi
AEP (MWh)	3353.68	5786.03	3588.15	1342.87	5316.35	3091.99
CF (%)	25.5	44	27.3	10.2	40.4	23.5
Model Type	**Vestas-3000**					
Study	**Our Proposed Model**			**Study in Ref. [41]**		
Site	Q. A. Airport	K. H. Airport	Safawi	Q. A. Airport	K. H. Airport	Safawi
AEP (MWh)	7445.04	13132.92	8056.58	2014.31	7974.53	4657.99
CF (%)	27.6	48.8	29.9	9.8	37.4	19.6

The model described in this study can be used at any wind site in the world. To implement the wind distribution with a high level of precision, it just requires high-resolution wind speed data. This can be calculated using data from the nearest meteorological station to the intended wind site, adjusted to the proposed wind farm's hub height.

9. Real Measurements and Validations Process

Since Q_3 model has provided the minimum *LCoE*, as shown in Table 7, only this model will be validated with real measurements data. Therefore, a comparison study has been established between the measured energy output obtained from several wind farms in Jordan and the estimated value based on the exponential power model (Q_3) for the corresponding wind farms. Table 9 shows the measured data of four wind farms operated in Jordan for the year 2019. The data, which are provided by the National Electric Power Company (NEPCO), includes the total energy production of the wind farm, its capacity

factor, and the cost per unit of energy. The technical specifications of these wind farms are presented in Table 9.

Table 9. The measured output data and the technical specifications of the wind farms.

Year	**2019**			
Month	**Tafila (MWh)**	**Hussein (MWh)**	**Al-Rajaf (MWh)**	**Al-Fajeej (MWh)**
Jan	44,405	14,720	30,830	3645
Feb	33,818	11,785	26,105	0
Mar	38,770	14,045	24,961	0
Apr	31,352	12,544	27,645	0
May	26,251	9334	19,461	0
Jun	30,315	7214	22,840	0
Jul	31,433	5748	23,151	17,908
Aug	28,968	4260	21,693	26,363
Sep	17,583	2357	12,660	18,566
Oct	16,526	3748	13,862	10,656
Nov	25,437	3646	20,160	20,400
Dec	37,692	9944	30,968	22,473
Total	362,550	99,345	274,336	120,011
CF	35.4%	14.2%	36.4%	15.4%
Cost (JD/MWh)	85	80	80	83
Wind Farm Specifications				
Wind Farm Name	**Turbine Model**	**Hub Height (m)**	**Capacity (MW)**	**No. of Turbines**
Tafila	Vestas (V112/3.075)	94/84	117	38
Al–Hussein Uni.	Gamesa (G97/2.0)	78	80	40
Al-Rajaf	Gamesa (G114/2.1)	80	86.1	41
Al-Fajeej	Vestas (V126/3.3)	117	89.1	27

The average wind speed data required for this analysis are provided by the National Energy Research Center (NERC). These data, which are recorded at different heights, are corrected to the hub height of the wind farms using (74).α, which represents the wind shear exponent selected to be 0.15 for all wind farms as open terrain areas. The corrected wind speeds are also presented in Table 10.

Table 10. The monthly mean wind speeds of the wind farms.

Month	Tafila			Al-Hussein Uni.		Al-Rajaf		Al-Fajeej	
	v_{ref} (45m)	v_{hub} (94m)	v_{hub} (84m)	v_{ref} (51m)	v_{hub} (78m)	v_{ref} (50m)	v_{hub} (80m)	v_{ref} (50m)	v_{hub} (117m)
Jan	10.69	11.51	11.38	6.64	6.93	6.58	6.9	7.08	7.71
Feb	9.23	9.94	9.82	7.48	7.8	6.94	7.27	8.05	8.76
Mar	9.69	10.43	10.31	7.22	7.53	6.44	6.75	6.67	7.26
Apr	9.08	9.77	9.66	5.5	5.74	6.25	6.55	6.78	7.38
May	7.82	8.42	8.32	6.29	6.56	6.85	7.18	6.41	6.98
Jun	8.16	8.78	8.69	6.87	7.17	6.74	7.06	7.1	7.73
Jul	7.79	8.39	8.29	6.84	7.14	5.91	6.19	5.88	6.4
Aug	7.6	8.18	8.09	5.93	6.19	6.53	6.84	6.47	7.04
Sep	6.28	6.76	6.68	5.81	6.06	6.2	6.5	5.2	5.66
Oct	5.86	6.31	6.24	4.56	4.76	5.78	6.06	5.09	5.54
Nov	8.86	9.54	9.43	4.02	4.19	6.23	6.53	5.52	6.01
Dec	9.38	10.1	9.98	5.24	5.47	7.07	7.41	6.71	7.31

Rayleigh distribution, which is a simplified model of Weibull distribution and depends only on the average wind speed of the wind sites, is utilized to perform this analysis to keep consistency with the available wind data. The complete derivation of wind energy extracted by the turbines based on the Rayleigh exponential power model (R-Q_3) is derived in this section. The probability distribution function PDF of Rayleigh in terms of mean wind speed V_m can be written, as follows [43].

$$f_R(v) = \frac{\pi}{2}\left(\frac{v}{{V_m}^2}\right)e^{-\frac{\pi}{4}(\frac{v}{V_m})^2} \tag{39}$$

The estimated energy produced by wind turbines based on the exponential power model (6) is given by the following formula.

$$E_{est} = (1-\mu) \times T\left(\int_{v_i}^{v_r} Q_3(v) f_R(v)\ dv + \int_{v_r}^{v_o} P_R f_R(v)\ dv\right) \tag{40}$$

where, μ is the total turbine losses, which is assumed to be 15%. Substituting (6) and (39) in (40) yields the following:

$$E_{est} = \frac{(1-\mu)\ \pi\ TP_R}{2\ {V_m}^2}\left(\int_{v_i}^{v_r} ve^{-\frac{\pi}{4}(\frac{v}{V_m})^2}dv - \int_{v_i}^{v_r} ve^{-\frac{\pi}{4}(\frac{v}{V_m})^2-(\frac{v}{\beta})^5}dv + \int_{v_r}^{v_o} ve^{-\frac{\pi}{4}(\frac{v}{V_m})^2}dv\right) \tag{41}$$

Evaluating the integrals in first and third terms in (6). Thus, the estimated energy produced using (Q_3) and Rayleigh model can be expressed, as follows.

$$E_{est} = \frac{(1-\mu)\ \pi\ TP_R}{2\ {V_m}^2}\left[\frac{2\ {V_m}^2}{\pi}\left(e^{-\frac{\pi}{4}(\frac{v_i}{V_m})^2} - e^{-\frac{\pi}{4}(\frac{v_o}{V_m})^2}\right) - \int_{v_i}^{v_r} ve^{-\frac{\pi}{4}(\frac{v}{V_m})^2-(\frac{v}{\beta})^5}dv\right] \tag{42}$$

The estimated capacity factor of selected wind farms has been estimated by (16). Error analysis is performed between the measured and estimated energy produced, which can be expressed, as follows [43].

$$Error\ (\%) = \left|\frac{E_{mes} - E_{est}}{E_{est}}\right| \times 100\% \tag{43}$$

The estimated cost per unit energy *LCoE* is calculated using Life Cycle Cost (LCC) method. The capital cost for each turbine model is evaluated based on modified NREL's cost model. The input parameters of the analysis are presented in Table 11.

Table 11. The input parameters of the analysis.

Parameter	Tafila	Al-Hussein Uni.	Al-Rajaf	Al-Fajeej
Cut—in speed (v_i)	2.5	3	1	3
Rated speed(v_r)	13	14	11.5	12
Cut—out speed (v_o)	25	25	25	22.5
Wind Shear Exponent	0.1	0.1	0.1	0.1
Cost Scaling Factor	2.03	1.54	1.46	1.39
Economic Input Parameters				
Discount rate (r) for 2019	4% [79]			
Inflation rate (i) for 2019	0.3% [80]			
O & M percentage (f_{OM})	3.5%			
Lifetime of system (N)	20 years			

Table 12 presents the results for the comparison study between the measured output data and the estimated data based on (R-Q_3) model for the selected wind farms. The error analysis shows that Al-Rajaf wind farm achieves the lowest percentage error with around 6.16%, followed by Al-Fajeej and Tafila Wind farms which recorded 13.03% and 18.18%, respectively. The worst result was achieved by Al-Hussein University wind farm with an error value of around 20%. Regarding the estimated *CF* results, Tafila wind farm recorded the highest value of around 42%. All results obtained in this comparison study are provided in Table 12.

Table 12. The technical comparison between the measured and estimated output data of the farms.

Site	Tafila				Al-Hussein Uni.			
Month	E_{mes}	E_{est}	CF_{est}	*Error(%)*	E_{mes}	E_{est}	CF_{est}	*Error(%)*
Jan	44,405	46,589.81	53.59	4.92	14,720	14,646.19	24.61	0.5
Feb	33,818	37,664.58	47.97	11.37	11,785	16,722.98	31.11	41.9
Mar	38,770	43,522.91	50.06	12.26	14,045	17,345.31	29.14	23.5
Apr	31,352	39,685.5	47.17	26.58	12,544	8866.606	15.39	29.32
May	26,251	34,339.02	39.5	30.81	9334	12,937.44	21.74	38.61
Jun	30,315	35,147.79	41.78	15.94	7214	15,231.99	26.44	111.14
Jul	31,433	34,168.33	39.3	8.7	5748	15,603.9	26.22	171.47
Aug	28,968	32,954.05	37.91	13.76	4260	11,220.85	18.85	163.4
Sep	17,583	22,899.66	27.22	30.24	2357	10,278.15	17.84	336.07
Oct	16,526	20,440.06	23.51	23.68	3748	5073.311	8.52	35.36
Nov	25,437	38,723.56	46.03	52.23	3646	3058.701	5.31	16.11
Dec	37,692	42,325.31	48.69	12.29	9944	7964.85	13.38	19.9
Total E_{est}	428,460.6				138,950.28			
Total E_{mes}	362,550				111,345			

Table 12. *Cont.*

Site		**Tafila**				**Al-Hussein Uni.**		
Month	E_{mes}	E_{est}	CF_{est}	*Error(%)*	E_{mes}	E_{est}	CF_{est}	*Error(%)*
Error(%)		18.18				19.6		
Overall CF_{est}		41.86				19.83		
Overall CF_{mes}		35.4				14.2		
$LCOE_{est}$		71.92				112.56		
$LCOE_{mes}$		119.89				112.84		
Site		**Al-Rajaf**				**Al-Fajeej**		
Month	E_{mes}	E_{est}	CF_{est}	*Error(%)*	E_{mes}	E_{est}	CF_{est}	*Error(%)*
Jan	30,830	22,634.64	35.33	26.58	3645	5907.97	39.08	36.8
Feb	26,105	22,151.01	38.28	15.15	18,166	14,151.1	22.06	23.78
Mar	24,961	21,836.63	34.09	12.52	10,256	13,898.58	20.97	30.43
Apr	27,645	20,076.21	32.39	27.38	20,100	16,181.2	25.22	20.68
May	19,461	24,075.23	37.58	23.71	22073	23,950.95	36.13	6.58
Jun	22,840	22,708.84	36.63	0.57	27,645	20,076.21	32.39	27.38
Jul	23,151	18,709.04	29.21	19.19	17,908	19,004.12	28.67	6.12
Aug	21,693	22,317.59	34.84	2.88	26,363	22,549.87	34.02	14.46
Sep	12,660	19,807.69	31.95	56.46	18,566	14,151.1	22.06	23.78
Oct	13,862	17,953.33	28.03	29.51	10,656	13,898.58	20.97	30.43
Nov	20,160	19,969.01	32.21	0.95	20,400	16,181.2	25.22	20.68
Dec	30,968	25,209.15	39.35	18.6	22,473	23,950.95	36.13	6.58
Total E_{est}		257,448.36				135,643.8		
Total E_{mes}		274,336				120,011		
Error(%)		6.16				13.03		
Overall CF_{est}		34.13				17.38		
Overall CF_{mes}		36.4				15.4		
$LCOE_{est}$		75.58				141.07		
$LCOE_{mes}$		112.84				117.07		

10. Conclusions

This paper proposed a method for estimating the extracted energy of wind farms using several mathematical models. The developed models include five turbine models and three wind distribution models. They were used to suggest suitable wind turbines with specific features for wind farms to be installed in nine potential wind sites in Jordan, which are: Queen Alia Airport, Amman Civil Airport, King Hussein Airport, Irbid, Mafraq, Ma'an, Safawi, Irwaished and Ghor Es Safi. The suggested wind farms achieved maximum extracted energy, maximum capacity factor and minimum Levelized Cost of Energy. The whale optimization algorithm was used to solve the developed optimization problem. The results showed that King Hussein Airport achieves the best results among other sites by recording the minimum LCoE and maximum CF with values of 33.81 USD/MWh and 0.54, respectively.

The developed model with Q_3 and Rayleigh distribution function was validated with real measurements data from several wind farms in Jordan. Error analysis showed that the difference between the measured and estimated energy is less than 20%. The study has validated the provided a model which can now be utilized routinely for the assessment of wind energy potential in a specific wind site. Moreover, the model is very useful to estimate the wind potential before the wind farm is built, so that a decision can be made on the type of wind turbine that can be used.

The limitations of this methodology can be divided into two main parts. The first one is the accuracy of the wind speed representation using the distribution function, which is mainly dependent on the resolution of the wind speed data. The second one is the accuracy of estimation of the correction factor of the National Renewable Energy Laboratory (NREL) modified cost model, which is mainly dependent on the actual cost of the wind project.

Author Contributions: A.A.-Q. suggested the idea for the paper, wrote several sections of the paper, reviewed and edited the paper before the final submission. B.A.-M. wrote several parts of the paper and derived the mathematical model described in the paper. All authors have read and agreed to the published version of the manuscript.

Funding: This research received no external funding.

Institutional Review Board Statement: Not applicable.

Informed Consent Statement: Not applicable.

Data Availability Statement: The data were provided by Taqs Alarab Company and National Electric Power Company (NEPC).

Acknowledgments: The authors acknowledge Yarmouk University, Taqs Alarab Company and National Electric Power Company (NEPC) for their support in this study.

Conflicts of Interest: The authors declare no conflict of interest.

References

1. De Castro, M.; Salvador, S.; Gómez-Gesteira, M.; Costoya, X.; Carvalho, D.; Sanz-Larruga, F.J.; Gimeno, L. Europe, China and the United States: Three different approaches to the development of offshore wind energy. *Renew. Sustain. Energy Rev.* **2019**, *109*, 55–70. [CrossRef]
2. Calif, R.; Schmitt, F. Modeling of atmospheric wind speed sequence using a lognormal continuous stochastic equation. *J. Wind Eng. Ind. Aerodyn.* **2012**, *109*, 1–8. [CrossRef]
3. Sathyajith, M. *Wind Energy: Fundamentals, Resource Analysis and Economics*; Springer: Berlin/Heidelberg, Germany, 2006.
4. Ko, D.H.; Jeong, S.T.; Kim, Y.C. Assessment of wind energy for small-scale wind power in Chuuk State, Micronesia. *Renew. Sustain. Energy Rev.* **2015**, *52*, 613–622. [CrossRef]
5. Han, Q.; Ma, S.; Wang, T.; Chu, F. Kernel density estimation model for wind speed probability distribution with applicability to wind energy assessment in China. *Renew. Sustain. Energy Rev.* **2019**, *115*, 109387. [CrossRef]
6. Ladenburg, J.; Hevia-Koch, P.; Petrović, S.; Knapp, L. The offshore-onshore conundrum: Preferences for wind energy considering spatial data in Denmark. *Renew. Sustain. Energy Rev.* **2020**, *121*, 109711. [CrossRef]
7. Peters, J.L.; Remmers, T.; Wheeler, A.J.; Murphy, J.; Cummins, V. A systematic review and meta-analysis of GIS use to reveal trends in offshore wind energy research and offer insights on best practices. *Renew. Sustain. Energy Rev.* **2020**, *128*, 109916. [CrossRef]
8. Rosales-Asensio, E.; Borge-Diez, D.; Blanes-Peiró, J.-J.; Pérez-Hoyos, A.; Comenar-Santos, A. Review of wind energy technology and associated market and economic conditions in Spain. *Renew. Sustain. Energy Rev.* **2019**, *101*, 415–427. [CrossRef]
9. Carrillo, C.; Obando Montaño, A.F.; Cidrás, J.; Díaz-Dorado, E. Review of power curve modelling for wind turbines. *Renew. Sustain. Energy Rev.* **2013**, *21*, 572–581. [CrossRef]
10. Jiang, H.; Wang, J.; Wu, J.; Geng, W. Comparison of numerical methods and metaheuristic optimization algorithms for estimating parameters for wind energy potential assessment in low wind regions. *Renew. Sustain. Energy Rev.* **2017**, *69*, 1199–1217. [CrossRef]
11. Wang, J.; Hu, J.; Ma, K. Wind speed probability distribution estimation and wind energy assessment. *Renew. Sustain. Energy Rev.* **2016**, *60*, 881–899. [CrossRef]
12. Pishgar-Komleh, S.H.; Keyhani, A.; Sefeedpari, P. Wind speed and power density analysis based on Weibull and Rayleigh distributions (a case study: Firouzkooh county of Iran). *Renew. Sustain. Energy Rev.* **2015**, *42*, 313–322. [CrossRef]
13. Wu, J.; Wang, J.; Chi, D. Wind energy potential assessment for the site of Inner Mongolia in China. *Renew. Sustain. Energy Rev.* **2013**, *21*, 215–228. [CrossRef]

14. Jung, C.; Schindler, D. Wind speed distribution selection—A review of recent development and progress. *Renew. Sustain. Energy Rev.* **2019**, *114*, 109290. [CrossRef]
15. Genç, M.S.; Çelik, M.; Karasu, İ. A review on wind energy and wind–hydrogen production in Turkey: A case study of hydrogen production via electrolysis system supplied by wind energy conversion system in Central Anatolian Turkey. *Renew. Sustain. Energy Rev.* **2012**, *16*, 6631–6646. [CrossRef]
16. Yeom, J.-M.; Deo, R.C.; Adamwoski, J.F.; Chae, T.; Kim, D.-S.; Han, K.-S.; Kim, D.-Y. Exploring solar and wind energy resources in North Korea with COMS MI geostationary satellite data coupled with numerical weather prediction reanalysis variables. *Renew. Sustain. Energy Rev.* **2019**, *119*, 109570. [CrossRef]
17. Elsner, P. Continental-scale assessment of the African offshore wind energy potential: Spatial analysis of an under-appreciated renewable energy resource. *Renew. Sustain. Energy Rev.* **2019**, *104*, 394–407. [CrossRef]
18. Chen, X.; Foley, A.; Zhang, Z.; Wang, K.; O'Driscoll, K. An assessment of wind energy potential in the Beibu Gulf considering the energy demands of the Beibu Gulf Economic Rim. *Renew. Sustain. Energy Rev.* **2019**, *119*, 109605. [CrossRef]
19. Kazimierczuk, A.H. Wind energy in Kenya: A status and policy framework review. *Renew. Sustain. Energy Rev.* **2019**, *107*, 434–445. [CrossRef]
20. Li, Y.; Huang, X.; Tee, K.F.; Li, Q.; Wu, X.-P. Comparative study of onshore and offshore wind characteristics and wind energy potentials: A case study for southeast coastal region of China. *Sustain. Energy Technol. Assess.* **2020**, *39*, 100711. [CrossRef]
21. Bilir, L.; İmir, M.; Devrim, Y.; Albostan, A. Seasonal and yearly wind speed distribution and wind power density analysis based on Weibull distribution function. *Int. J. Hydrog. Energy* **2015**, *40*, 15301–15310. [CrossRef]
22. Chang, T.P. Estimation of wind energy potential using different probability density functions. *Appl. Energy* **2011**, *88*, 1848–1856. [CrossRef]
23. Boudia, S.M.; Benmansour, A.; TabetHellal, M.A. Wind resource assessment in Algeria. *Sustain. Cities Soc.* **2016**, *22*, 171–183. [CrossRef]
24. Azad, K.; Mohammad, R.; Halder, P.; Sutariya, J. Assessment of Wind Energy Prospect by Weibull Distribution for Prospective Wind Sites in Australia. *Energy Procedia* **2019**, *160*, 348–355. [CrossRef]
25. Gugliani, G.K.; Sarkar, A.; Ley, C.; Mandal, S. New methods to assess wind resources in terms of wind speed, load, power and direction. *Renew. Energy* **2018**, *129*, 168–182. [CrossRef]
26. Saeed, M.A.; Ahmed, Z.; Yang, J.; Zhang, W. An optimal approach of wind power assessment using Chebyshev metric for determining the Weibull distribution parameters. *Sustain. Energy Technol. Assess.* **2020**, *37*, 100612. [CrossRef]
27. Alrashidi, M.; Rahman, S.; Pipattanasomporn, M. Metaheuristic optimization algorithms to estimate statistical distribution parameters for characterizing wind speeds. *Renew. Energy* **2020**, *149*, 664–681. [CrossRef]
28. Dong, Y.; Wang, J.; Jiang, H.; Shi, X. Intelligent optimized wind resource assessment and wind turbines selection in Huitengxile of Inner Mongolia, China. *Appl. Energy* **2013**, *109*, 239–253. [CrossRef]
29. Wang, J.; Huang, X.; Li, Q.; Ma, X. Comparison of seven methods for determining the optimal statistical distribution parameters: A case study of wind energy assessment in the large-scale wind farms of China. *Energy* **2018**, *164*, 432–448. [CrossRef]
30. Aries, N.; Boudia, S.M.; Ounis, H. Deep assessment of wind speed distribution models: A case study of four sites in Algeria. *Energy Convers. Manag.* **2018**, *155*, 78–90. [CrossRef]
31. Al-Quraan, A.; Stathopoulos, T.; Pillay, P. Comparison of Wind Tunnel and on Site Measurements for Urban Wind Energy Estimation of Potential Yields. *J. Wind Eng. Ind. Aerodyn.* **2016**, *158*, 1–10. [CrossRef]
32. Stathopoulos, T.; Alrawashdeh, H.; Al-Quraan, A.; Blocken, B.; Dilimulati, A.; Paraschivoiu, M.; Pillay, P. Urban Wind Energy: Some Views on Potential and Challenges. *J. Wind Eng. Ind. Aerodyn.* **2018**, *179*, 146–157. [CrossRef]
33. Al-Quraan, A.; Pillay, P.; Stathopoulos, T. Use of a Wind Tunnel for Urban Wind Power Estimation. In Proceedings of the IEEE Power & Energy Society General Meeting, Washington, DC, USA, 27–31 July 2014.
34. Al-Quraan, A.; Stathopoulos, T.; Pillay, P. Estimation of Urban Wind Energy-Equiterre Building Case in Montreal. In Proceedings of the International Civil Engineering for Sustainability and Resilience Conference (CESARE'14), Irbid, Jordan, 24–27 April 2014.
35. Alsaad, M. Wind energy potential in selected areas in Jordan. *Energy Convers. Manag.* **2013**, *65*, 704–708. [CrossRef]
36. Bataineh, K.M.; Dalalah, D. Assessment of wind energy potential for selected areas in Jordan. *Renew. Energy* **2013**, *59*, 75–81. [CrossRef]
37. Khraiwish Dalabeeh, A.S. Techno-economic analysis of wind power generation for selected locations in Jordan. *Renew. Energy* **2017**, *101*, 1369–1378. [CrossRef]
38. Anani, A.; Zuamot, S.; Abu-Allan, F.; Jibril, Z. Evaluation of wind energy as a power generation source in a selected site in Jordan. *Sol. Wind Technol.* **1988**, *5*, 67–74. [CrossRef]
39. Habali, S.M.; Hamdan, M.A.S.; Jubran, B.A.; Zaid, A.I.O. Wind speed and wind energy potential of Jordan. *Sol. Energy* **1987**, *38*, 59–70. [CrossRef]
40. Amr, M.; Petersen, H.; Habali, S. Assessment of wind farm economics in relation to site wind resources applied to sites in Jordan. *Sol. Energy* **1990**, *45*, 167–175. [CrossRef]
41. Ammari, H.D.; Al-Rwashdeh, S.S.; Al-Najideen, M.I. Evaluation of wind energy potential and electricity generation at five locations in Jordan. *Sustain. Cities Soc.* **2015**, *15*, 135–143. [CrossRef]

42. Al-Quraan, A.; Alrawashdeh, H. Correlated Capacity Factor Strategy for Yield Maximization of Wind Turbine Energy. In Proceedings of the IEEE 5th International Conference on Renewable Energy Generation and Applications (ICREGA), Al-Ain, United Arab Emirates, 26–28 February 2018.
43. Al-Quraan, A.; Al-Mahmodi, M.; Hussein, A.R.; Al-Masri, M.K. Comparative study between measured and estimated wind energy yield. *Turk. J. Electr. Eng. Comp. Sci.* **2020**, *28*, 2926–2939. [CrossRef]
44. Al-Quraan, A.; Al-Qaisi, M. Modelling, Design and Control of a Standalone Hybrid PV-Wind Micro-Grid System. *Energies* **2021**, *14*, 4849. [CrossRef]
45. Al-Mhairat, B.; Al-Quraan, A. Assessment of Wind Energy Resources in Jordan Using Different Optimization Techniques. *Processes* **2022**, *10*, 105. [CrossRef]
46. Blanco, M.I. The economics of wind energy. *Renew. Sustain Energy Rev.* **2009**, *13*, 1372–1382. [CrossRef]
47. Manwell, J.F.; McGowan, J.G.; Rogers, A.L. *Wind Energy Explained: Theory, Design and Application*, 2nd ed.; Wiley & Sons: Hoboken, NJ, USA, 2010.
48. Nelson, V.; Starcher, K. *Wind Energy: Renewable Energy and the Environment*, 3rd ed.; CRC Press: Boca Raton, FL, USA, 2018.
49. Perkin, S.; Garrett, D.; Jensson, P. Optimal wind turbine selection methodology: A case-study for Búrfell, Iceland. *Renew. Energy* **2015**, *75*, 165–172. [CrossRef]
50. Rezaei Mirghaed, M.; Roshandel, R. Site specific optimization of wind turbines energy cost: Iterative approach. *Energy Convers. Manag.* **2013**, *73*, 167–175. [CrossRef]
51. Fingersh, L.J.; Hand, M.M.; Laxson, A.S. *Wind Turbine Design Cost and Scaling Model*; National Renewable Energy Laboratory: Golden, CO, USA, 2006.
52. Letcher, T.M. *Wind Energy Engineering: A Handbook for Onshore and Offshore Wind Turbines*, 1st ed.; Academic Press: Cambridge, MA, USA, 2017.
53. Radaideh, A.; Bodoor, M.; Al-Quraan, A. Active and Reactive Power Control for Wind Turbines Based DFIG Using LQR Controller with Optimal Gain-Scheduling. *J. Electr. Comp. Eng.* **2021**, *2021*, 1218236. [CrossRef]
54. Al-Quraan, A.; Al-Mahmodi, M.; Al-Asemi, T.; Bafleh, A.; Bdour, M.; Muhsen, H.; Malkawi, A. A New Configuration of Roof Photovoltaic System for Limited Area Applications—A Case Study in KSA. *Buildings* **2022**, *12*, 92. [CrossRef]
55. Walker, R.P.; Swift, A. *Wind Energy Essentials: Societal, Economic, and Environmental Impacts*, 1st ed.; Wiley & Sons: Hoboken, NJ, USA, 2015.
56. Eminoglu, U.; Turksoy, O. Power curve modeling for wind turbine systems: A comparison study. *Int. J. Ambient Energy* **2019**, *42*, 1912–1921. [CrossRef]
57. Stehly, T.; Beiter, P.; Duffy, P. *2019 Cost of Wind Energy Review*; National Renewable Energy Laboratory: Golden, CO, USA, 2020. Available online: https://www.nrel.gov/docs/fy21osti/78471.pdf (accessed on 23 January 2022).
58. Forbes, C.; Evans, M.; Hastings, N.; Peacock, B. *Statistical Distributions*, 4th ed.; Wiley & Sons: Hoboken, NJ, USA, 2010.
59. Bortolotti, P.; Berry, D.; Murray, R.; Gaertner, E.; Jenne, D.; Damiani, R.; Barter, G.; Dykes, K. *A Detailed Wind Turbine Blade Cost Model*; Technical Report NREL/TP-5000-73585; National Renewable Energy Laboratory: Golden, CO, USA, 2019. Available online: https://www.nrel.gov/docs/fy19osti/73585.pdf (accessed on 23 January 2022).
60. Shahab, S.; Lades, L. Sludge and transaction costs. *Behav. Public Policy*. 2021. pp. 1–22. Available online: https://www.cambridge.org/core/journals/behavioural-public-policy/article/sludge-and-transaction-costs/D09206BF9B36C129F40A27A9E749074B (accessed on 23 January 2022).
61. Cavusoglu, S.S.; Macário, R. Minimum delay or maximum efficiency? Rising productivity of available capacity at airports: Review of current practice and future needs. *J. Air Transp. Manag.* **2021**, *90*, 101947. [CrossRef]
62. Foryś, I.; Głuszak, M.; Konowalczuk, J. Compensation due to land use restrictions: The case of limited use area in the vicinity of Polish airports. *Oecon. Copernic.* **2019**, *10*, 649–667. [CrossRef]
63. Masdar Co. Tafilah Wind Farm. 2021. Available online: https://masdar.ae/en/masdar-clean-energy/projects/tafila-wind-farm (accessed on 23 January 2022).
64. Elecnor Group. Al-Rajef Wind Farm. 2021. Available online: https://www.elecnor.com/resources/files/1/projects/en/referencia-al-rajef-wind-farm-jordan-en.pdf (accessed on 23 January 2022).
65. Alcazar Energy. Al-Rajef Wind Farm. 2021. Available online: https://alcazarenergy.com/wp-content/uploads/2021/01/Project-Fact-Sheets_Al-Rajef-86MW.pdf (accessed on 23 January 2022).
66. KOSPO Co-Funds $101 m 51.75 MW Wind Farm in Jordan. (2 October 2018). 2021. Available online: https://asian-power.com/project/news/kospo-co-funds-101m-5175mw-wind-farm-in-jordan (accessed on 23 January 2022).
67. IFC Funds New Wind Power Plant in Jordan. (7 November 2018). 2021. Available online: https://www.petra.gov.jo/Include/InnerPage.jsp?ID=11309&lang=en&name=en_news (accessed on 23 January 2022).
68. Ministry of Energy and Mineral Resources—Jordan. Daihan Wind Project. 2021. Available online: https://www.memr.gov.jo/Ar/NewsDetails/%D8%B2%D9%88%D8%A7%D8%AA%D9%8A_%D8%AA%D8%AF%D8%B4%D9%86_%D9%85%D8%B4%D8%B1%D9%88%D8%B9_%D8%AF%D8%A7%D9%8A%D9%87%D8%A7%D9%86_%D9%84%D8%B7%D8%A7%D9%82%D8%A9_%D8%A7%D9%84%D8%B1%D9%8A%D8%A7%D8%AD_%D9%81%D9%8A_%D8%A7%D9%84%D8%B7%D9%81%D9%8A%D9%84%D8%A9 (accessed on 23 January 2022).
69. Alcazar Energy. Shobak Wind Farm. 2021. Available online: https://alcazarenergy.com/wp-content/uploads/2021/01/Project-Fact-Sheets_Shobak-Wind.pdf (accessed on 23 January 2022).

70. Jordan's Fujeij Wind Energy Project Inaugurated. (16 October 2019). 2021. Available online: https://www.evwind.es/2019/10/16/jordans-fujeij-wind-energy-project-inaugurated/71345 (accessed on 23 January 2022).
71. Korea's KEPCO Opens 89-MW Wind Park in Jordan. (17 October 2019). 2021. Available online: https://renewablesnow.com/news/koreas-kepco-opens-89-mw-wind-park-in-jordan-672962/ (accessed on 23 January 2022).
72. Elecnor Co. Ma'an Wind Farm. 2021. Available online: https://www.elecnor.com/resources/files/1/projects/en/referencia-maan-jordan-en.pdf (accessed on 23 January 2022).
73. Wind Energy in Jordan, Awards Siemens Gamesa Contract for 80 MW Wind Farm. (24 July 2019). 2021. Available online: https://www.evwind.es/2019/11/24/wind-energy-in-jordan-awards-siemens-gamesa-contract-for-80-mw-wind-farm/71984 (accessed on 23 January 2022).
74. Ministry of Energy and Mineral Resources—Jordan. Ma'an Wind Farm. 2021. Available online: https://www.memr.gov.jo/Ar/NewsDetails/%D8%A7%D9%81%D8%AA%D8%AA%D8%A7%D8%AD_%D9%85%D8%B4%D8%B1%D9%88%D8%B9_%D8%B7%D8%A7%D9%82%D8%A9_%D8%A7%D9%84%D8%B1%D9%8A%D8%A7%D8%AD_%D9%81%D9%8A_%D9%85%D8%B9%D8%A7%D9%86 (accessed on 23 January 2022).
75. Wind Farms in Jordan. 2021. Available online: https://www.thewindpower.net/windfarms_list_en.php?country=JO (accessed on 23 January 2022).
76. Hu, J.; Harmsen, R.; Crijns-Graus, W.; Worrell, E. Geographical optimization of variable renewable energy capacity in China using modern portfolio theory. *Appl. Energy* **2019**, *253*, 113614. [CrossRef]
77. Gualtieri, G.; Secci, S. Methods to extrapolate wind resource to the turbine hub height based on power law: A 1-h wind speed vs. Weibull distribution extrapolation comparison. *Renew. Energy* **2012**, *43*, 183–200. [CrossRef]
78. Chen, J.; Wang, F.; Stelson, K.A. A mathematical approach to minimizing the cost of energy for large utility wind turbines. *Appl. Energy* **2018**, *228*, 1413–1422. [CrossRef]
79. Central Bank of Jordan, (15 December 2020). Central Bank Interest Rates. 2021. Available online: https://www.cbj.gov.jo/Pages/viewpage.aspx?pageID=259 (accessed on 23 January 2022).
80. Central Bank of Jordan, (4 February 2021). Economic Indicators. 2021. Available online: https://www.cbj.gov.jo/Pages/viewpage.aspx?pageID=282 (accessed on 23 January 2022).